

Supplementary material
to
Structural and functional characterization of the BcsG subunit of
the cellulose synthase in *Salmonella typhimurium*

by

**Lei Sun^{1*}, Peter Vella^{2*}, Robert Schnell², Anna Polyakova³,
Gleb Bourenkov³, Fengyang Li¹, Annika Cimdins¹, Thomas Schneider³, Ylva
Lindqvist², Michael Y. Galperin^{4**}, Gunter Schneider^{2**}, and Ute Römling^{1**}**

¹Department of Microbiology, Tumor and Cell Biology, Karolinska Institutet, S-171 77, Stockholm, Sweden;

²Department of Medical Biochemistry and Biophysics, Karolinska Institutet, S-171 77, Stockholm, Sweden;

³European Molecular Biology Laboratory, D-22607 Hamburg, Germany;

⁴National Center for Biotechnology Information, National Library of Medicine, National Institutes of Health, Bethesda, Maryland 20894, USA

This Supplementary Material includes 11 figures and 3 tables

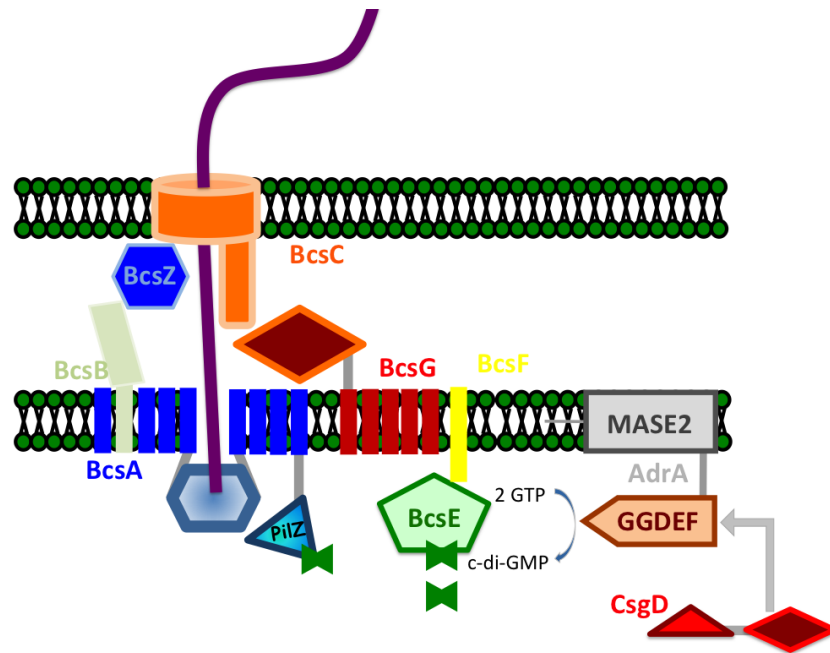


Figure S1. Proteins involved in cellulose biosynthesis and its regulation as mentioned in this work.

BcsA is the catalytic subunit of the cellulose synthase, which contains a C-terminal c-di-GMP binding PilZ domain and BcsB is a periplasmic protein with a C-terminal transmembrane helix required for *in vitro* cellulose biosynthesis. These two proteins constitute the active cellulose synthase [1]. BcsC is the predicted outer membrane pore and BcsZ is a periplasmic glycosyl hydrolase family 8 cellulase that reduces cellulose production [2, 3]. Accessory proteins are BcsE, a cytoplasmic c-di-GMP receptor [4], the short transmembrane protein BcsF and the alkaline phosphatase-related protein BcsG (this work, [5]). On agar plates, the orphan response regulator CsgD is required for amyloid curli and cellulose biosynthesis through activation of transcription of the diguanylate cyclase AdrA, which produces the c-di-GMP required for cellulose biosynthesis [6].

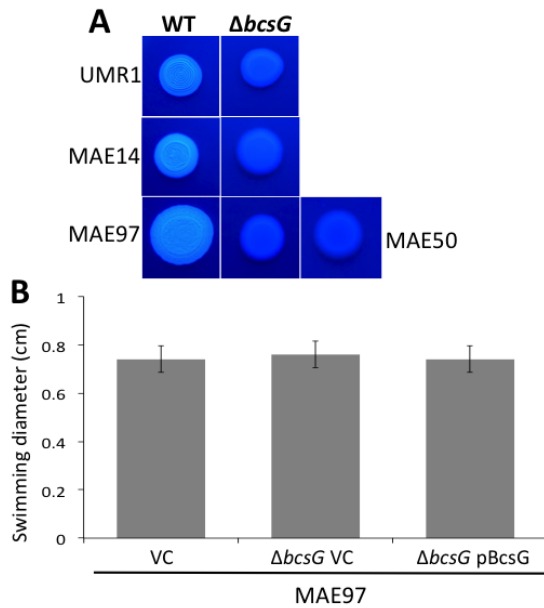


Figure S2. Calcofluor binding and motility of *S. typhimurium* ATCC14028-1s derivatives.

A. Calcofluor binding phenotypes of *S. typhimurium* strains UMR1 (cellulose⁺/curli⁺, 28 °C), MAE14 (cellulose⁺/curli⁻, 28 °C) and MAE97 (cellulose⁺/curli⁻, 28 °C/37 °C) and their respective $\Delta bcsG$ deletion mutants, observed using Calcofluor white fluorescence. Strain MAE50 ($\Delta csgD$) served as a negative control. Cells were grown on salt-free LB agar plates with 50 μ g/ml Calcofluor at 28 °C for 48 h. Wild type and mutant colonies are from the same plate.

B. Swimming motility of MAE97, its $\Delta bcsG$ mutant and the $\Delta bcsG$ mutant complemented with BcsG expressed from a plasmid (pBcsG). The swimming diameter was measured after 5 h of incubation on an LB agar plate with 0.3% agar at 28 °C.

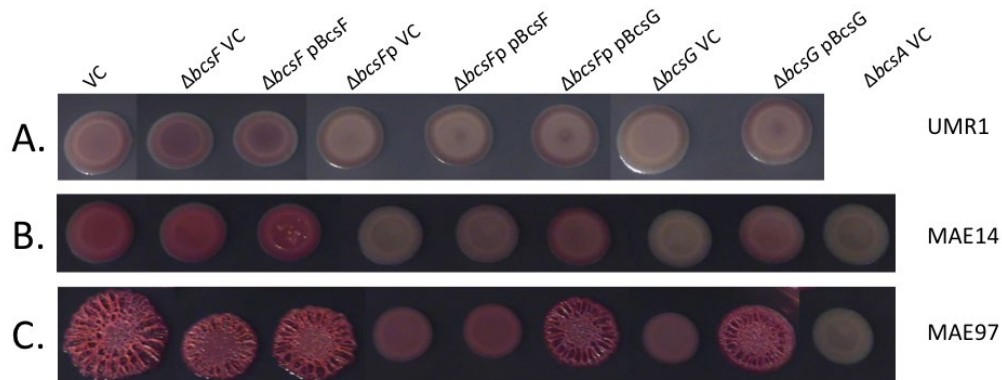


Figure S3. Colony morphotypes of polar and non-polar *bcsF* deletion mutants in *S. typhimurium* ATCC14028-1s derivatives.

Colony morphotypes of *S. typhimurium* strains UMR1 (cellulose⁺/curli⁺, 28 °C) (A), MAE14 (cellulose⁺, 28 °C) (B) and MAE97 (cellulose⁺, 28/37 °C) (C). The non-polar ($\Delta bcsF$) deletion mutants show a slightly reduced colony morphotype, which can be rescued by the expression of plasmid-borne *bcsF*. The polar ($\Delta bcsFp$) deletion mutants show a severely reduced colony morphotype resembling a *bcsG* mutant, which cannot be complemented by *bcsF* plasmid expression, but can be overcome by *bcsG* expression.

Vector control (VC) is plasmid pBAD30. pBcsF is wild-type *bcsF* with a C-terminal 6xHis-tag cloned in pBAD30. pBcsG is wild-type *bcsG* with a C-terminal 8xHis-tag cloned in pBAD30. $\Delta bcsA$ strain was used as negative control. Cells were grown on salt-free LB agar plates containing Congo red for 24 h at 28 °C. See Table S2 for the complete genotypes.

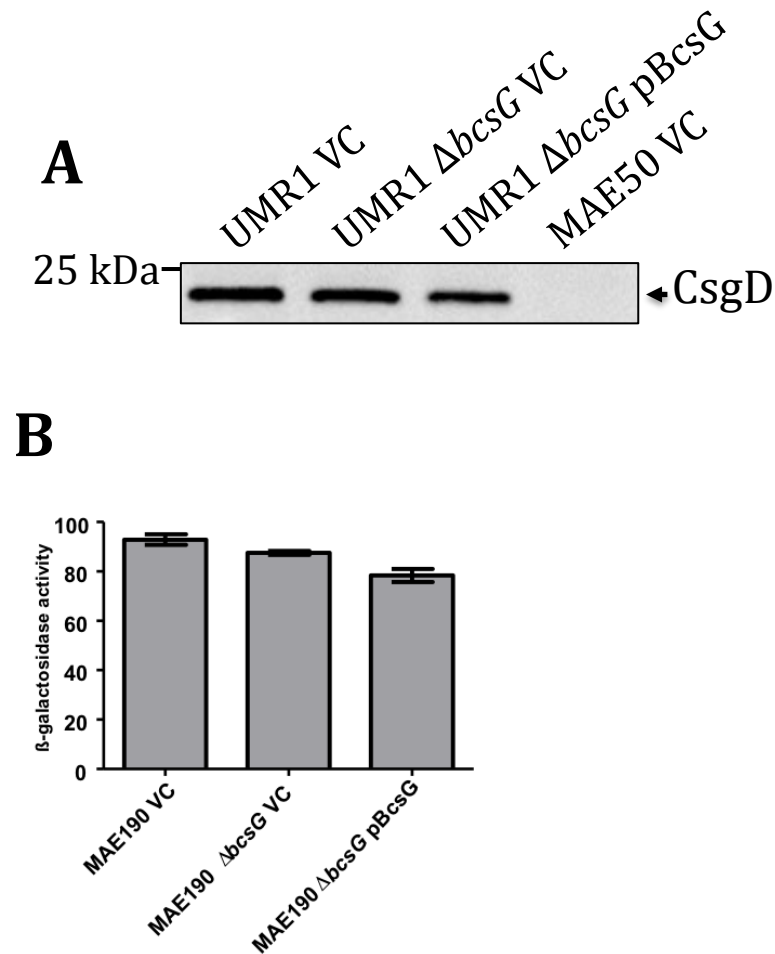


Figure S4. Production of the *rdar* biofilm activator CsgD and expression of the cellulose synthase BcsA are not regulated by BcsG.

A. Expression of CsgD in *S. typhimurium* UMR1 upon deletion or overexpression of *bcsG*. Cells were grown on salt-free LB agar for 24 h at 28 °C. VC indicates vector control pBAD30; pBcsG, wild-type *bcsG* cloned in pBAD30 with a C-terminal 8xHis tag. MAE50 is a *csgD* deletion mutant used as negative control. Western blot analysis with anti-CsgD antiserum (1:5000 dilution) has been performed as described [6].

B. Transcription of the *bcsA* gene encoding the cellulose synthase catalytic subunit is not affected by deletion or overexpression of *bcsG* as measured by β -galactosidase activity expressed from a *bcsA*::MudJ fusion construct. Cells were grown on salt-free LB agar for 24 h at 28 °C and resuspended in cold working buffer adjusted to OD₆₀₀=0.1. MAE190 contains a *bcsA101*::MudJ insertion in strain MAE97. VC and pBcsG constructs are as in panel A. See Table S2 for the complete genotypes.

A. Alignment of the N-terminal membrane portion and the linker region of BcsG proteins from *S. typhimurium* and other bacteria. Uncharged residues are shaded yellow, conserved aromatic residues forming a predicted 'aromatic belt' along the membrane surface [7] are in bold, Arg and Lys are in blue, Asp and Glu are in red. Conserved Lys31 and Asp82 in the hydrophobic core are marked with asterisks. The proteins are listed under their UniProt accession codes and abbreviated names of the respective genera. The source sequences are as follows: *Yersinia enterocolitica* LC20_00134 (GenBank accession number AHM71390); *Erwinia billingiae* EbC_43970 (CAX61928); *Klebsiella pneumoniae* KPN_03888 (ABR79275); *Proteus mirabilis* PMI2096 (CAR44189); *Serratia proteamaculans* Spro_0143 (ABV39253); *Pseudoalteromonas haloplanktis* PSHAa2158 (CAI87214); *Shewanella violacea* SVI_0134 (BAJ00105); *Vibrio fischeri* VF_A0887 (AAW87957); *Photobacterium profundum* PBPRA1716 (CAG20123); *Frateuria aurantia* Fraau_2360 (AFC86727); *Pseudomonas stutzeri* PST_0283 (ABP77989); *Pseudomonas putida* PP_2632 (AAN68240); *Chromobacterium violaceum* CV_2673 (AAQ60343); *Sutterella wadsworthensis* BN489_01704 (CCZ17195); *Leptothrix cholodnii* Lcho_2073 (ACB34340); *Burkholderia pseudomallei* BPSS1576 (CAH39049), and *Cupriavidus metallidurans* Rmet_2257 (ABF09136).

B. Predicted membrane topology of BcsG drawn by Protter (<http://wlab.ethz.ch/protter/>, [8]). Positions of the intramembrane Lys31 and Asp82 are marked with blue and red circles, respectively.

C. Alignment of the membrane portions of *S. typhimurium* BcsG protein and lipid A phosphoethanolamine transferase from *Neisseria meningitidis* (NmEptA, PDB entry 5FGN [7]). The alignment was constructed based on the results of an HHpred [9] search and reconciling the predicted secondary structures and membrane topologies of the two proteins. Coloring is as in panel A, secondary structure elements (predicted for BcsG and derived from the 5FGN structure using the DSSP algorithm [10]) are as follows: H, α -helix; E, β -strand; C, coil; T, turn. Identical residues are marked with asterisk, similar residues with the plus signs.

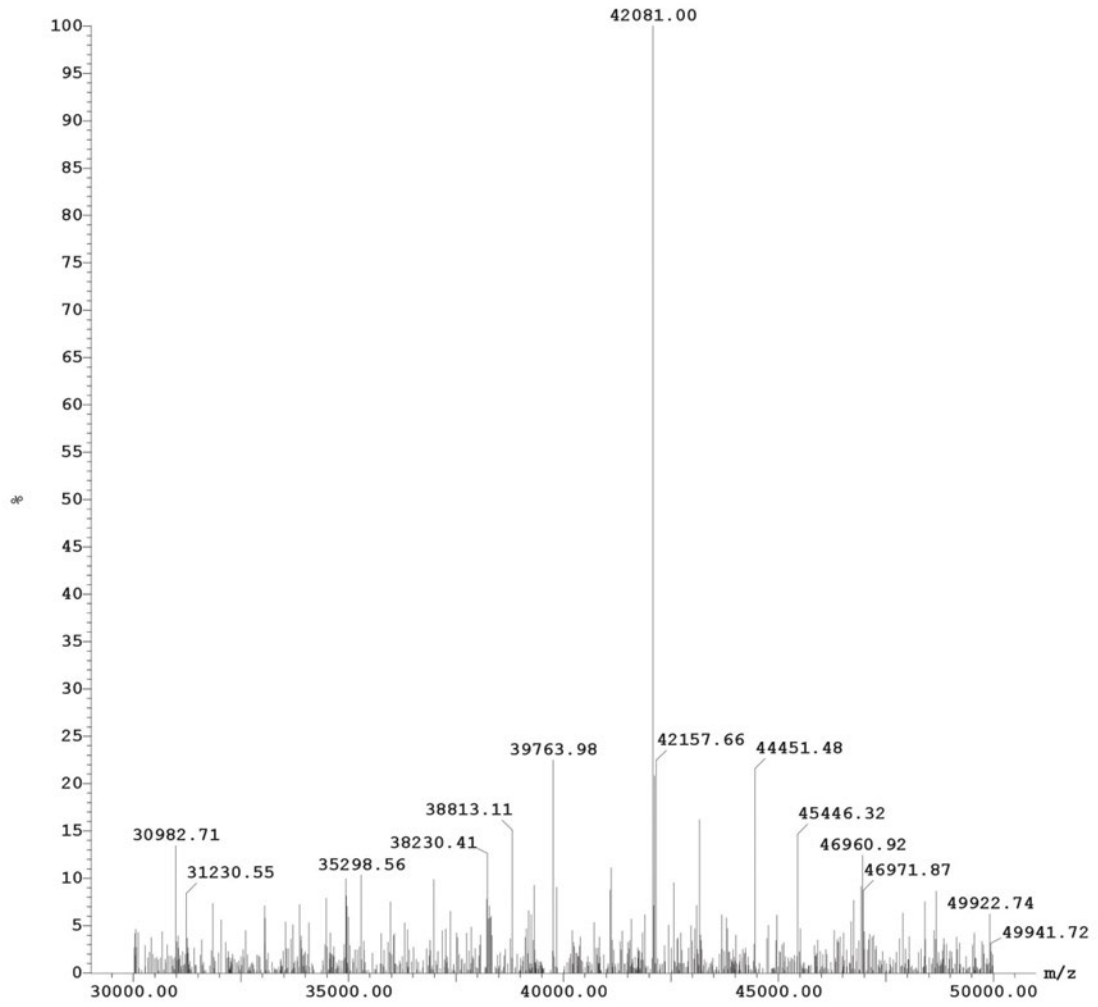


Figure S6. Mass-spectrum of the purified BcsG construct after cleavage with factor Xa.

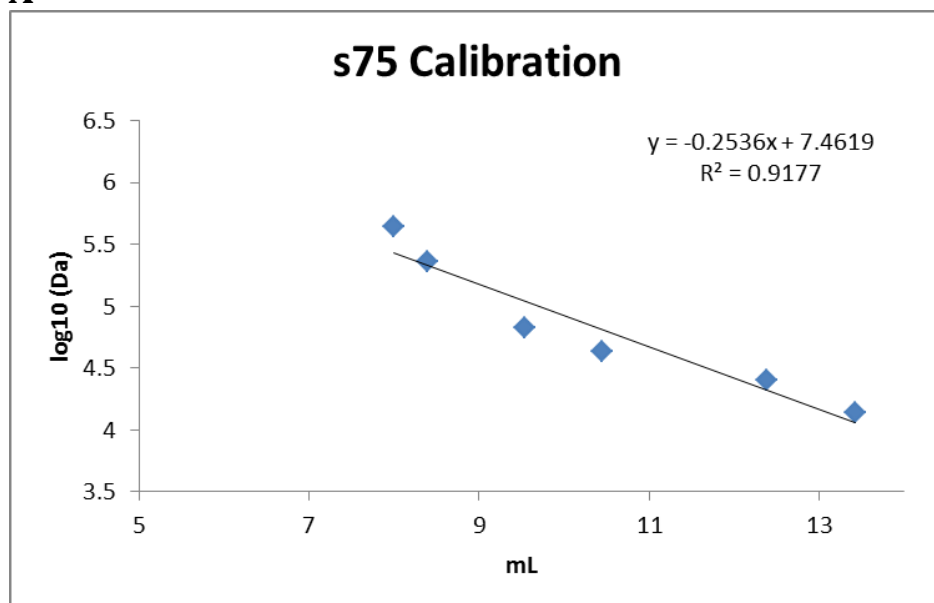
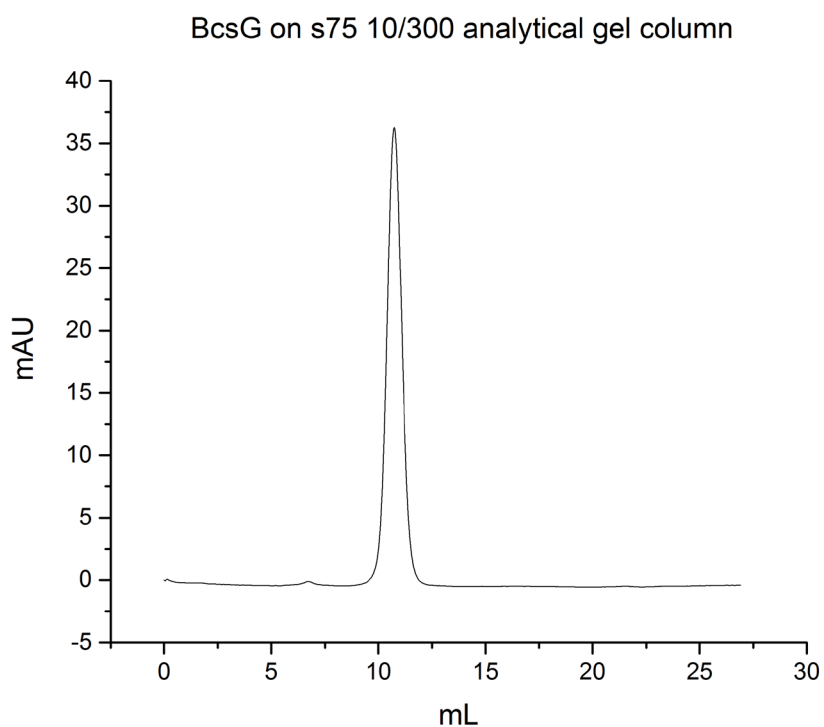
A**B**

Figure S7. Analytical gel chromatography of the purified BcsG construct after tag cleavage used in the crystallization experiments.

A. Calibration curve obtained with ribonuclease-A (13.7 kDa), chymotrypsinogen-A (25 kDa), ovalbumin (43 kDa), albumin (67 kDa), catalase (232 kDa), ferritin (440 kDa) and Blue Dextran (2 MDa).

B. Elution profile of purified BcsG. BcsG elutes as a monomer.

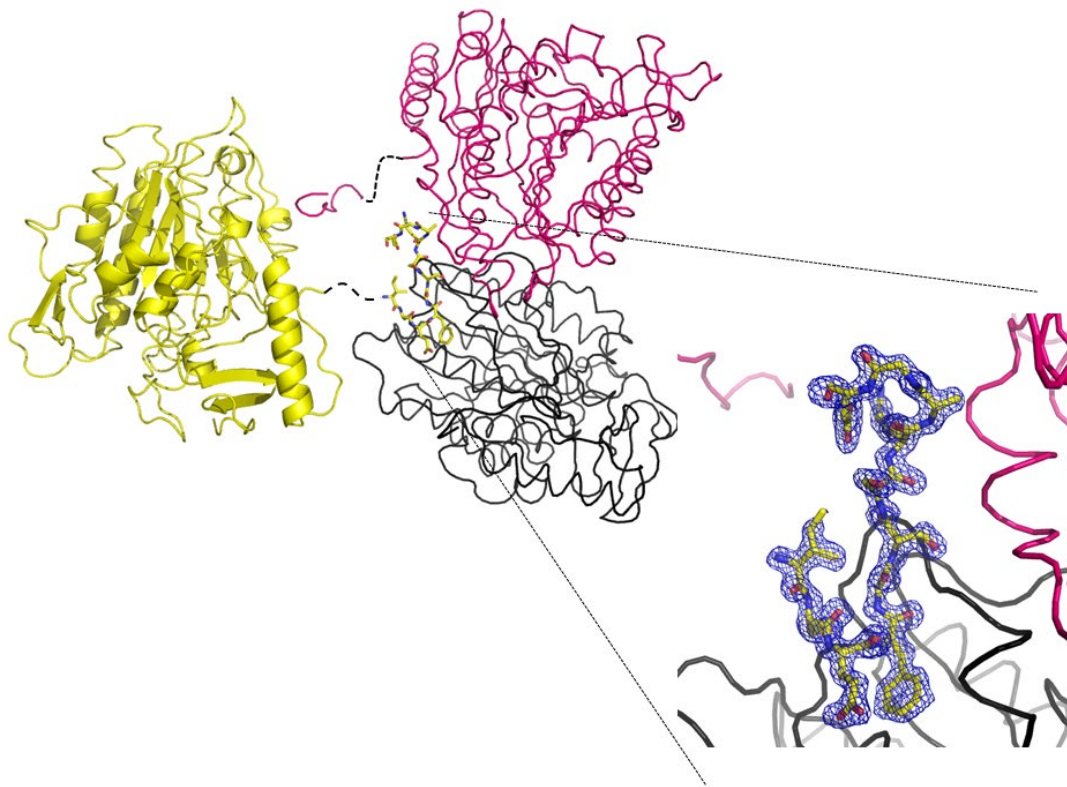


Figure S8. Crystal packing interactions of the tag-derived linker peptide with a neighboring BcsG molecule in the crystal lattice. Part of the 2Fo-Fc electron density map, contoured at 1.5σ , at the position of the bound peptide derived from the maltose binding protein tag is shown. The side chain of linker residue Phe4 is buried into a small pocket of the neighboring BcsG molecule and forms van-der-Waals interactions with the aliphatic parts of the side chains of Arg503 and Lys519. Other important interactions are made through hydrogen bonds of the carbonyl oxygen atom of Phe4 with the peptide amide group of Asn516, the amide nitrogen and side chain hydroxyl group of the linker Ser6 residue with the side chain of Glu512, and the amide nitrogen atom of linker Ser2 residue with the carbonyl oxygen atom of Ser514. In total, this packing interface contributes with 300 \AA^2 of buried surface area to the packing interactions between two symmetry related molecules.

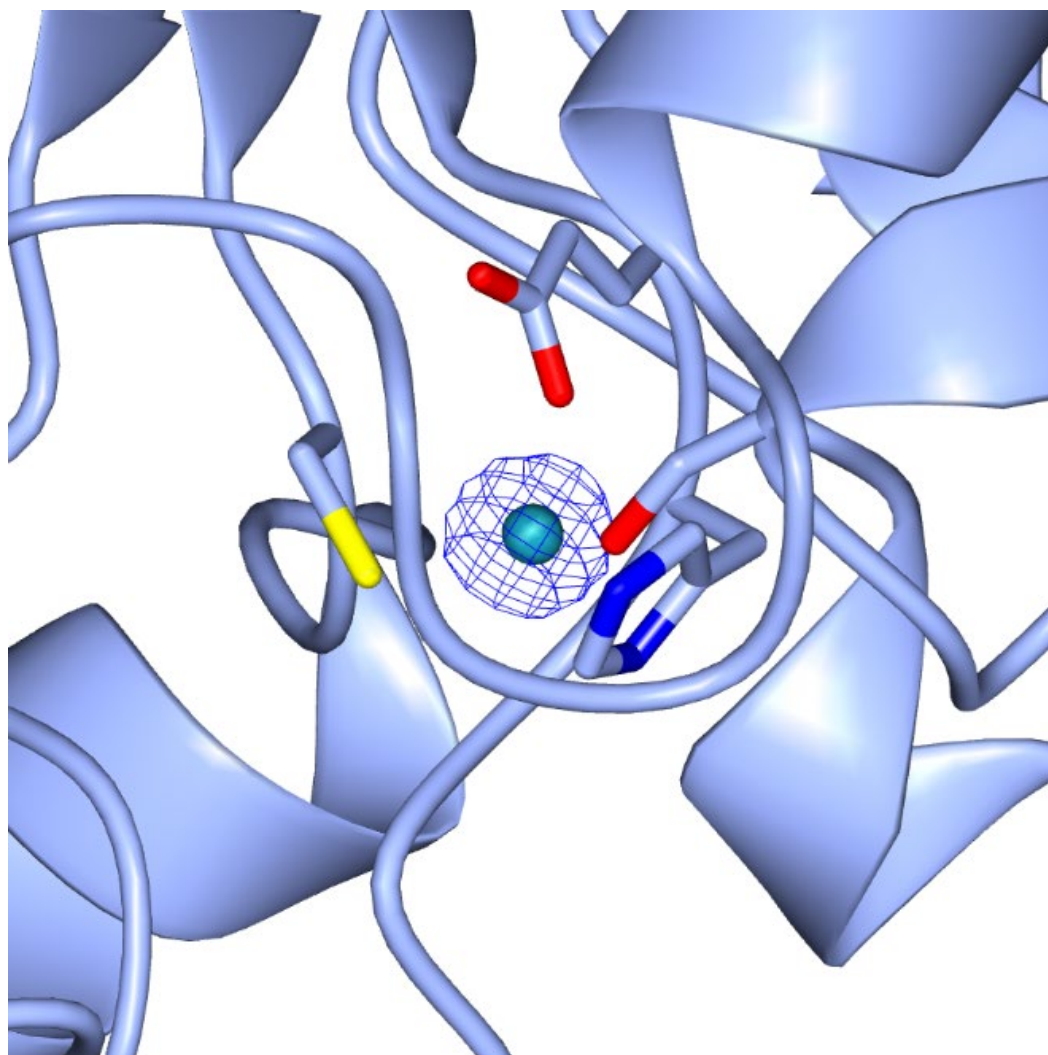
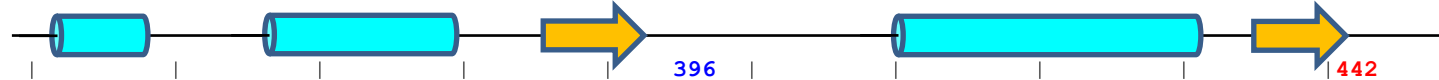


Figure S9. Anomalous difference electron density map at the metal binding site of BcsG contoured at 15σ , demonstrating that the bound metal in this site is a Zn^{2+} ion. The electron density map was calculated based on the X-ray data collected at the absorption edge of Zn^{2+} ($\lambda = 1.278 \text{ \AA}$).



BcsG St	234	PFDLLV	INIC	CSLS	WSDVEA	AAGLMSH	PLWSH	EDILF	KHFN	SGT	SGPAA	IRLLR	RASCG	QPSH	TRLYQ	PANNE	CYLF	DNLAK	L	GF	TQHL	L	M	D	H	N	G	E	328																																																													
BcsG Ec	234	PFELLV	INIC	CSLS	WSDIEA	AAGLMSH	PLWSH	EDIEF	KNFN	SATS	SGPAA	IRLLR	RASCG	QTSHT	NLYQ	PANNC	CYLF	DNLSK	L	GF	TQHL	L	M	G	H	N	G	N	Q	328																																																												
BcsG Cv	202	GFDVLL	LHV	CSLS	WDDLRA	VGF	DNPL	LARE	DIVF	DRFN	SAASY	SGPAA	LRVLR	RASCG	QPRHS	ALYEP	PAPE	QCFL	FENL	AKAG	FKTEL	S	L	N	H	D	G	S	296																																																													
PF11658	193	PFDLLV	LNI	CSLS	WDDLDA	AGLRNH	PLWKR	EDIVF	DNFN	SATS	SGPAA	IRLLR	RASCG	QPSHS	SDLYQ	PAPQC	CYLF	DNLAK	L	GF	TQQL	L	M	N	H	D	G	H	287																																																													
3lxq Vp	85	RKNLVIL	LQ	ESL	GAQFV	GS	GLG	2LT	PNL	DEL	4WQ	FTQ	X	YAT	G	TR	S	VRG	IEAV	T	G	F	P	P	S	P	S	R	A	3	185																																																											
4uop Lm	57	GKNLIIV	QLE	ESF	QRNLT	NV	KIN	3IT	P	LDG	6SN	QFF	Q	T	V	S	K	S	N	T	A	D	A	E	W	S	V	Y	T	S	T	F	P	S	G	Y	2	159																																																				
5i5d St	259	GQNVLL	ITV	D	GLN	YSR	F	E	K	---	Q	M	E	L	A	T	F	4I	D	F	T	R	H	X	S	S	G	N	T	2	D	N	G	I	F	G	L	F	Y	G	-	I	S	P	G	Y	D	-	-	V	L	S	T	R	T	P	A	A	L	I	T	A	L	N	Q	Q	G	Y	Q	L	G	L	F	S	S	D	G	-	-	348										
4upl Sp	17	VMNILF	I	M	F	D	Q	L	R	W	D	Y	L	S	C	Y	G	H	3N	T	P	H	I	D	R	L	4V	R	F	D	R	A	I	Q	S	P	I	C	G	S	S	R	M	S	T	Y	T	G	R	V	H	S	H	G	A	3	G	I	P	L	K	V	G	E	M	T	M	G	D	H	L	R	A	A	G	M	G	C	W	L	V	G	-	-	-	-	113			
5g2t Bt	23	KPNFLI	I	Q	C	D	H	L	T	Q	R	V	V	G	A	Y	G	Q	4T	L	P	I	D	E	V	A	3V	I	F	S	N	A	Y	V	G	C	P	L	S	Q	P	S	R	A	L	W	S	G	M	P	H	Q	T	N	V	R	S	N	S	E	P	V	N	P	T	L	G	S	L	F	S	E	S	G	Y	E	A	V	H	F	G	K	-	-	-	-	125			
2w8d Bc	31	GKNVIY	V	S	L	E	S	L	Q	S	F	I	I	D	Y	K	I	D	3V	T	P	F	L	N	K	I	8F	D	N	F	F	H	Q	T	G	Q	G	K	T	S	D	A	E	F	X	X	E	N	S	L	Y	P	L	A	Q	G	S	2	V	N	K	A	Q	N	T	L	Q	S	V	P	A	I	L	K	S	K	N	Y	T	S	A	T	F	H	G	N	T	Q	T	135
4uor Lm	60	GKNVIY	I	H	L	E	S	F	Q	Q	F	L	V	N	Y	K	L	N	3V	T	P	F	I	N	S	E	F	K	D	Q	N	T	L	S	3	G	Q	G	K	T	A	D	S	E	M	L	L	E	N	S	L	Y	G	L	P	Q	G	S	2	T	T	K	Q	N	T	Y	E	S	A	S	A	I	L	G	Q	Q	Y	T	S	A	V	F	H	G	N	Y	K	S	164	
5lrn Ec	21	PRLVVF	V	V	V	G	E	T	A	R	A	D	H	V	S	F	N	G	3T	F	P	Q	L	A	K	I	3T	N	F	S	N	V	T	S	C	G	T	S	T	A	Y	S	V	P	C	M	F	S	Y	L	G	A	D	E	Y	D	-	-	-	V	D	T	A	K	Y	Q	E	N	V	L	D	T	L	D	R	L	G	V	S	I	L	W	R	D	N	S	D	S	116	
4tn0 Cj	17	KKLLVL	V	V	V	G	E	T	A	R	A	A	N	Y	S	L	G	G	3D	T	N	F	Y	T	K	3V	F	F	D	N	F	S	S	C	G	T	A	V	S	L	P	C	M	F	S	I	S	K	R	E	N	Y	S	-	-	-	-	-	-	S	E	F	Q	E	N	A	M	D	V	L	Y	K	T	G	V	D	A	A	F	D	N	N	S	G	110					
4kay Ng	22	RRFVVL	V	V	V	G	E	T	T	R	A	A	N	W	L	N	G	Y	3T	T	P	L	L	A	A	R	4V	N	F	P	Q	V	R	S	C	G	T	A	H	S	L	P	C	M	F	S	T	F	D	R	T	D	Y	D	-	-	E	I	K	A	E	H	Q	D	N	L	L	D	I	V	Q	R	A	G	V	E	V	T	W	L	E	N	D	S	G	117				
5mx9 Ec	21	PRLVVF	V	V	V	G	E	T	A	R	A	D	H	V	S	F	N	G	3T	F	P	Q	L	A	K	I	3T	N	F	S	N	V	T	S	C	G	T	S	T	A	Y	S	V	P	C	M	F	S	Y	L	G	A	D	E	Y	D	-	-	-	V	D	T	A	K	Y	Q	E	N	V	L	D	T	L	D	R	L	G	V	G	I	L	W	R	D	N	-	-	113		
5grr Ec	21	PRLVVF	V	V	V	G	E	T	A	R	A	D	H	V	S	F	N	G	3T	F	P	Q	L	A	K	I	3T	N	F	S	N	V	T	S	C	G	T	S	T	A	Y	S	V	P	C	M	F	S	Y	L	G	A	D	E	Y	D	-	-	-	V	D	T	A	K	Y	Q	E	N	V	L	D	T	L	D	R	L	G	V	S	I	L	W	R	D	N	-	-	113		
lfsu Hs	3	PHHLV	F	L	L	A	D	D	L	G	W	N	D	V	G	F	H	G	S	2R	T	P	H	L	D	A	L	3G	V	L	L	D	N	Y	T	Q	P	L	X	T	P	S	R	S	Q	L	L	T	G	R	Y	Q	I	R	T	G	L	9	P	S	C	V	L	D	E	K	L	P	Q	L	K	E	A	G	Y	T	T	H	M	V	G	K	W	H	L	G	108			
lauk Hs	2	PNIVL	I	F	A	D	D	L	G	Y	G	D	L	G	C	Y	H	3T	T	P	N	L	D	Q	L	4R	F	T	D	F	Y	V	P	V	S	L	X	T	P	S	R	A	A	L	L	T	G	R	L	P	V	R	M	G	M	9	R	G	G	L	P	L	E	E	V	T	V	A	E	V	L	A	R	G	Y	L	T	G	M	A	G	K	W	H	L	G	109			
lei6 Pf	15	SAPTIV	I	C	V	D	G	C	E	Q	E	Y	I	N	Q	A	I	2Q	A	P	F	L	A	E	L	3G	T	V	L	T	G	D	2	V	P	S	F	T	N	P	N	L	S	I	V	T	G	A	P	P	S	V	H	G	1	7	N	D	A	K	Y	L	R	A	P	T	I	L	A	E	M	A	K	A	G	Q	L	V	A	V	T	A	K	D	K	-	127			
ly6v Ec	42	AKNIIL	L	I	G	D	G	M	G	D	S	E	I	T	A	A	R	N	7F	F	K	G	I	D	A	L	PL	T	G	Q	Y	T	H	1	2	V	T	D	S	A	A	S	A	T	A	W	S	T	G	V	K	T	Y	N	G	A	L	G	V	D	I	H	E	K	D	H	P	T	I	L	E	M	A	K	A	A	G	L	A	T	G	N	V	S	T	A	E	L	Q	152
PF00884	1	-PNVVL	V	L	V	L	G	E	S	L	R	A	P	D	L	G	L	Y	3T	T	P	F	L	D	R	L	3G	L	L	F	S	N	F	2	G	G	L	T	A	P	S	R	F	A	L	L	T	G	L	P	P	H	N	F	G	S	4	P	I	G	L	P	R	T	E	P	S	L	P	D	L	L	K	R	A	G	Y	N	T	G	A	I	G	K	W	H	L	G	102	



BcsG St	329	FGGFL	K	E	V	R	E	N	G	G	22	V	Y	D	D	L	A	V	L	N	R	W	L	T	G	E	E	R	A	N	S	R	S	A	T	F	N	L	L	P	L	H	D	N	H	F	P	G	V	S	K	T	A	D	Y	K	I	R	A	Q	K	L	F	D	E	L	D	A	F	F	T	E	L	E	K	S	G	R	K	V	M	V	V	V	V	P	E	H	G	G	A	L	K	448	
BcsG Ec	329	FGGFL	K	E	V	R	E	N	G	G	22	V	Y	D	D	T	A	V	L	N	R	W	L	D	V	T	E	K	D	K	N	S	R	S	A	T	F	N	T	L	P	L	H	D	N	H	F	P	G	V	S	K	T	A	D	Y	K	A	R	A	Q	K	F	F	D	E	L	D	A	F	F	T	E	L	E	K	S	G	R	K	V	M	V	V	V	V	P	E	H	G	G	A	L	K	448
BcsG Cv	298	FDSFL	Q	I	R	R	N	G	R	22	I	Y	S	D	A	M	L	N	R	W	L	Q	R	L	Q	E	P	D	P	H	V	A	Y	Y	N	T	I	S	L	H	D	G	N	R	I	S	E	A	4	T	D	A	S	Y	K	Y	R	A	G	R	L	L	R	D	I	G	F	I	D	L	L	E	Q	D	H	R	K	M	I	L	L	L	V	P	E	H	G	A	A	L	R	419			
PF11658	289	FDNFL	Q	L	I	R	E	N	G	G	23	Y	D	D	L	A	V	L	N	R	W	L	Q	R	E	K	S	D	D	G	R	V	A	T	F	Y	N	T	I	S	L	H	D	G	N																																																		

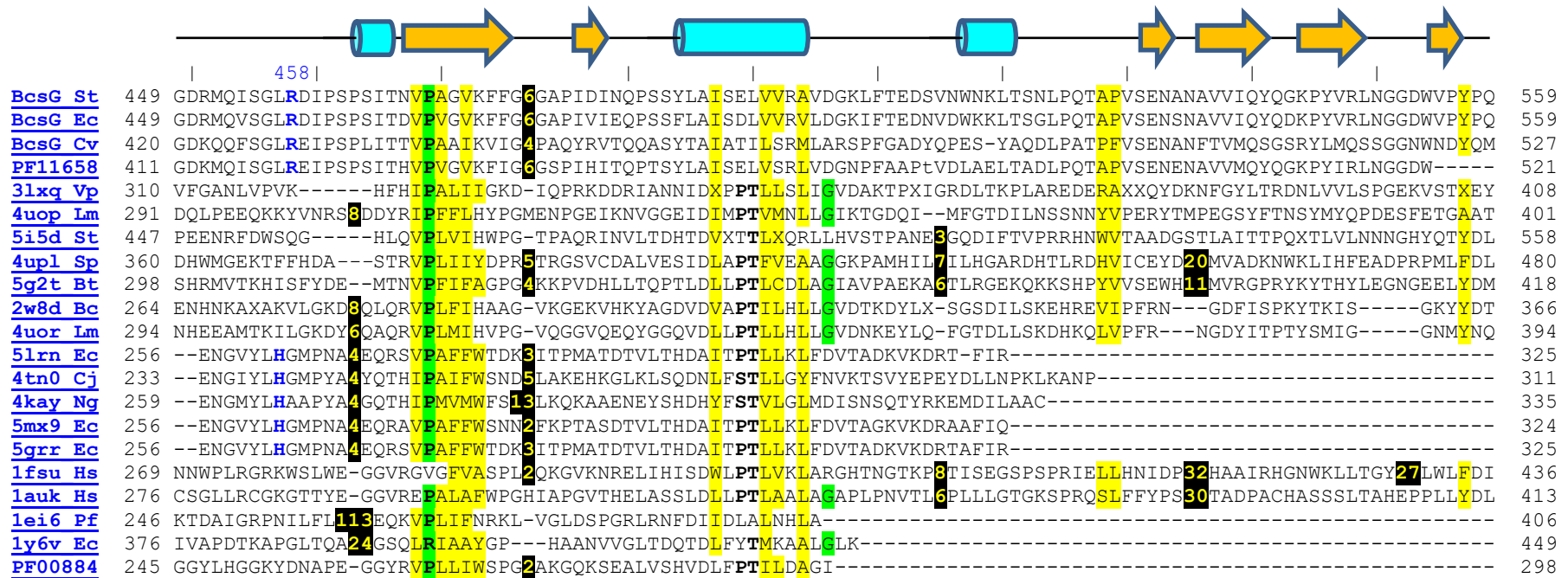


Figure S10. Structure-based sequence alignment of the C-terminal soluble domain of BcsG and related members of the alkaline phosphatase superfamily.

The top four rows include BcsG sequences from *S. typhimurium*, *E. coli*, and *Chromobacterium violaceum*, and from the Pfam domain PF11658, respectively. Subsequent rows include sequences of proteins with known structures, listed under their PDB identifiers and first letters of the genus and species names. All names are hyperlinked to the respective entries in the NCBI protein database. The last row shows the sequence of the Pfam domain Sulfatase (PF00884). The cylinders and arrows on the top indicate α -helices and β -strands, respectively, of the BcsG structure calculated using the DSSP algorithm [10], vertical bars mark each 10th residue. The active site residues are in bold and colored red (Asp, Glu) or blue (His, Asn). Conserved hydrophobic residues are shaded yellow, conserved turn residues (Gly, Pro) are shaded green. The alignment was constructed by reconciling structural alignments generated by the DALI [11] and VAST [12] tools.

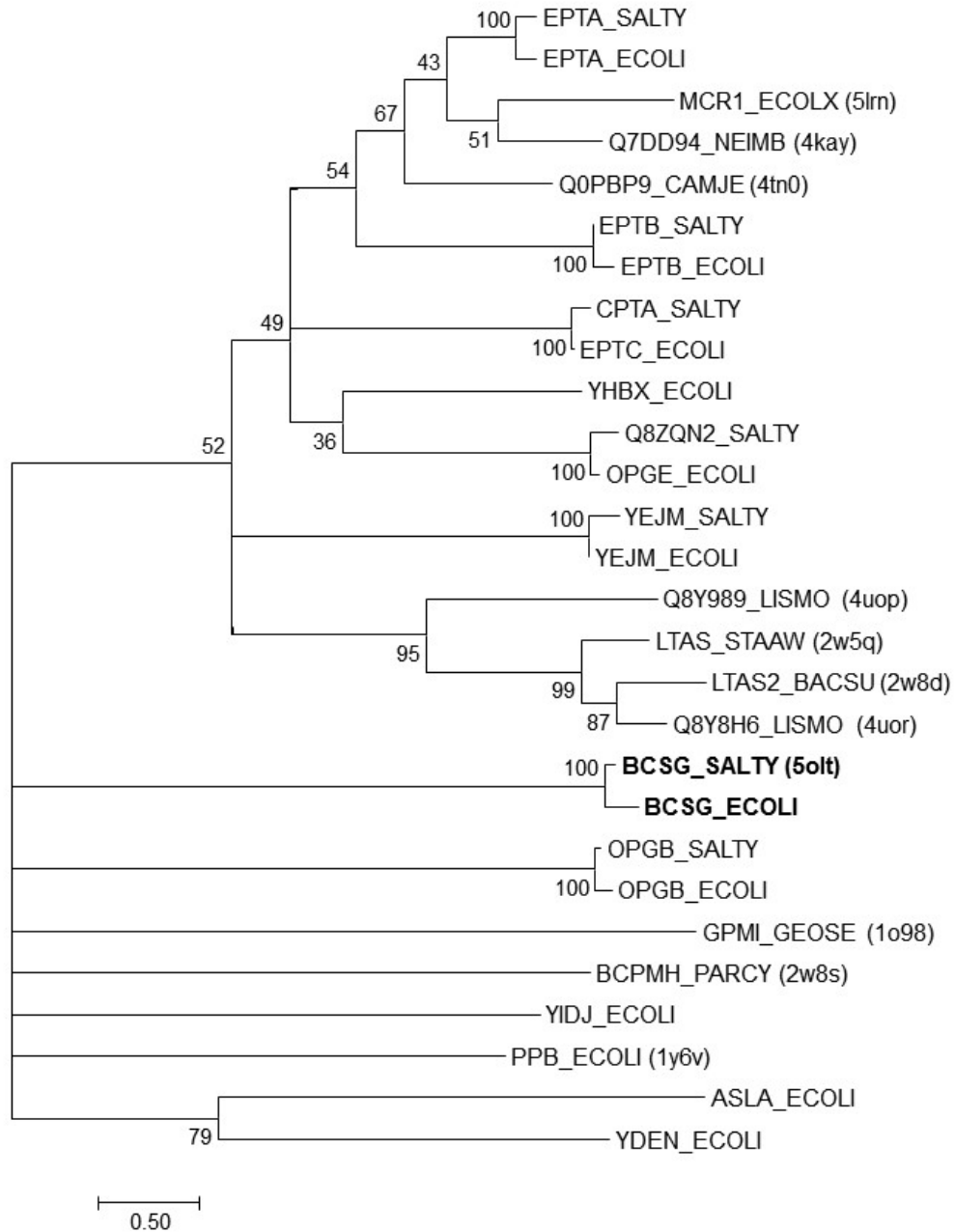


Figure S11. Maximum likelihood tree of phosphoethanolamine transferases from *E. coli*, *S. typhimurium* and related members of the alkaline phosphatase superfamily. Proteins are listed under their UniProt identifiers; PDB entries, where available, are shown in parentheses, see Tables 2 and S3 for details. The tree was constructed in MEGA7 [13] using the maximum likelihood method based on the JTT matrix-based model [14] with default parameters from an alignment built with MUSCLE [15]. All positions containing gaps were eliminated, leaving a total of 264 positions in the final dataset. The tree is drawn to scale, with branch lengths measured in the number of substitutions per site. The percentage of trees in which the associated taxa clustered together is shown next to the branches; those branches with <30% support have been collapsed.

Table S1. Strains and plasmids used in this study

Strain or plasmid	Relevant genotype or description	Reference/ Source
<i>E. coli</i> K-12		
DH5 α	$\lambda\phi 80dlacZ \Delta M15 \Delta(lacZYA-argF)U169$ <i>recA1 endA1 hsdR17(rK - mK -) supE44</i> <i>thi-1 gyrA relA1</i>	New England Biolabs
<i>S. Typhimurium</i> ATCC 14028 derivatives		
UMR1	ATCC14028-1s Nal^r , cellulose/curli fimbriae (<i>rdar</i>) 28 °C	[16]
MAE14	UMR1 $\Delta csgBA101::Km^r$, cellulose (<i>pdar</i>) 28°C	[6]
MAE50	UMR1 $\Delta csgD$	[6]
MAE52	UMR1 <i>pcsgD1</i> ; cellulose/curli fimbriae (<i>rdar</i>) 28/37 °C	[17]
MAE97	UMR1 <i>pcsgD1 \Delta csgBA102</i> , cellulose (<i>pdar</i>) 28/37 °C	[6]
MAE190	MAE97 <i>bcsA101::MudJ</i> cellulose/curli negative, (<i>saw</i>) 28/37 °C	[18]
MAE1264	MAE97 <i>bcsA-3xFLAG</i>	[19]
MAE1873	UMR1 <i>bcsC-3xFLAG Km</i>	[19]
MAE2201	UMR1 $\Delta bcsF::Cm$	This study
MAE2202	UMR1 $\Delta bcsF::tetRA$	This study
MAE2204	MAE14 $\Delta bcsF::Cm$	This study
MAE2205	MAE14 $\Delta bcsF::tetRA$	This study
MAE2207	MAE97 $\Delta bcsF::Cm$	This study
MAE2207	MAE97 $\Delta bcsF::tetRA$	This work
MAE2203	UMR1 $\Delta bcsG101$	This study
MAE2206	MAE14 $\Delta bcsG101$	This study
MAE2209	MAE97 $\Delta bcsG101$	This study
MAE2211	MAE1264 $\Delta bcsG101$	This study
MAE2215	UMR1 $\Delta bcsG-3xFLAG Km$	This study
MAE2217	UMR1 $\Delta bcsG101 bcsC-3xFLAG Km$	This study
Plasmids		
pBAD30	pACYC184 ori; L-arabinose regulated <i>araC</i> ; PBAD promoter; Amp^r	[20, 21]
pLAFR3	<i>IncP Tc^r cos⁺ rlx⁺</i>	[22]
pKD3	FRT-cat-FRT; Cm^r , Amp^r	[23]
pKD46	ParaB $\alpha\beta\gamma$; Amp^r	[23]
pSUB11	template for 3xFLAG-Km	[24]
pBAD-BcsF	<i>bcsF</i> cloned in <i>XbaI/HindIII</i> sites in pBAD30 with a 8xHis-Tag	This study
pBAD-BcsG	<i>bcsG</i> cloned in <i>XbaI/HindIII</i> sites in pBAD30 with a 8x His-Tag	This study

pBAD-BcsG _{C243S}	pBAD30-BcsG _{C243S} -8xHis	This study
pBAD-BcsG _{E442A}	pBAD30-BcsG _{E442A} -8xHis	This study
pBAD-BcsG _{S278A}	pBAD30-BcsG _{S278A} -8xHis	This study
pBAD-BcsG _{H396A}	pBAD30-BcsG _{H396A} -8xHis	This study
pBAD-BcsG _{H443A}	pBAD30-BcsG _{H443A} -8xHis	This study
pBAD-BcsG _{S493A}	pBAD30-BcsG _{S493A} -8xHis	This study
pBAD-BcsG ₁₋₁₆₅	pBAD30-BcsG (1-165 aa)-8xHis	This study
pBAD-BcsG ₁₋₂₁₀	pBAD30-BcsG (1-210 aa)-8xHis	This study
pMAL-c2x	MBP fusion overexpression vector; plac,Amp ^r	New England Biolabs
pMAL-BcsG1	pMAL-c2x-BcsG1 (185-559 aa)	This study
pMAL-BcsG2	pMAL-BcsG1 _{S278A}	This study
pWJB9 (pAdrA)	pLAFR3:: <i>araC PBAD adrA</i>	[25]

BcsGR458M_F	GAATGCAGATCTCAGGCCTGATGGATATTCCCAGCCCCTCCATC
BcsGR458M_R	GATGGAGGGGCTGGGAATATCCATCAGGCCTGAGATCTGCATTC
BcsGR458H_F	GCAGATCTCAGGCCTGCATGATATTCCCAGCCCCTC
BcsGR458H_R	GAGGGGCTGGGAATATCATGCAGGCCTGAGATCTGC
Cloning of <i>bcsG</i> in pMAL-c2 expression vector	
bcsGpMAL2-XbaIF	GTATCTAGA GCGGGCGATAAGCCGG
bcsGpMAL2-HindIIIR	TACAAGCTTTTACTGCGGGTAAGGCAC

Table S3. Phosphoethanolamine transferase family enzymes in *S. typhimurium*

Protein name	UniProt entry, accession	<i>S. typhimurium</i> LT2 locus tag	TM domain length ^b	Active site residue	Reference
Phosphoethanolamine transferase					
Cellulose biosynthesis protein BcsG	BCSG_SALTY, Q7CPI7	STM3624	162 aa, 5 TM	Ser	[5]; this work
Phosphoethanolamine transferase EptA	EPTA_SALTY, P36555	STM4293	175 aa, 5 TM	Thr	[26, 27]
Kdo ₂ -lipid A phosphoethanolamine 7''-transferase EptB	EPTB_SALTY, P43666	STM3635	180 aa, 5 TM	Thr	[28]
Phosphoethanolamine transferase CptA	CPTA_SALTY, Q7CPC0	STM4118	174 aa, 5 TM	Thr	[29]
Integral membrane protein OpgE/YbiP	Q8ZQN2_SALTY, Q8ZQN2	STM0834	158 aa, 4 TM	Thr	[30]
Phosphoethanolamine transferase MCR-1 ^a	MCR1_ECOLX, A0A0R6L508	N/A ^a	178 aa, 5 TM	Thr	[31, 32]
Phosphoglycerol transferase					
Phosphoglycerol transferase OpgB	OPGB_SALTY, Q8ZJX6	STM4541	132 aa, 4 TM	Thr	[31-33]
No known enzymatic activity					
Cardiolipin transfer protein PbgA	YEJM_SALTY, P40709	STM2228	190 aa, 5 TM	N/A	[34]

^a – This protein and its Arg536->His variant have been detected in recent environmental isolates of *S. typhimurium* (not in strain LT2 or its derivatives) [31, 32].

^b – Transmembrane domain length and helices predictions are taken from UniProt and/or calculated using MEMSAT-SVM [35].

References

- [1] J.L. Morgan, J. Strumillo, J. Zimmer. Crystallographic snapshot of cellulose synthesis and membrane translocation. *Nature* 493 (2013) 181-186.
- [2] I. Ahmad, S.F. Rouf, L. Sun, A. Cimdins, S. Shafeeq, S. Le Guyon, M. Schottkowski, M. Rhen, U. Romling. BcsZ inhibits biofilm phenotypes and promotes virulence by blocking cellulose production in *Salmonella enterica* serovar Typhimurium. *Microb Cell Fact* 15 (2016) 177.
- [3] U. Romling, M.Y. Galperin. Bacterial cellulose biosynthesis: diversity of operons, subunits, products, and functions. *Trends Microbiol* (2015).
- [4] X. Fang, I. Ahmad, A. Blanka, M. Schottkowski, A. Cimdins, M.Y. Galperin, U. Romling, M. Gomelsky. GIL, a new c-di-GMP-binding protein domain involved in regulation of cellulose synthesis in enterobacteria. *Mol Microbiol* 93 (2014) 439-452.
- [5] W. Thongsomboon, D.O. Serra, A. Possling, C. Hadjineophytou, R. Hengge, L. Cegelski. Phosphoethanolamine cellulose: A naturally produced chemically modified cellulose. *Science* 359 (2018) 334-338.
- [6] U. Römling, M. Rohde, A. Olsen, S. Normark, J. Reinkoster. AgfD, the checkpoint of multicellular and aggregative behaviour in *Salmonella typhimurium* regulates at least two independent pathways. *Mol. Microbiol.* 36 (2000) 10-23.
- [7] A. Anandan, G.L. Evans, K. Condic-Jurkic, M.L. O'Mara, C.M. John, N.J. Phillips, G.A. Jarvis, S.S. Wills, K.A. Stubbs, I. Moraes, C.M. Kahler, A. Vrielink. Structure of a lipid A phosphoethanolamine transferase suggests how conformational changes govern substrate binding. *Proc. Natl. Acad. Sci. USA* 114 (2017) 2218-2223.
- [8] U. Omasits, C.H. Ahrens, S. Muller, B. Wollscheid. Protter: interactive protein feature visualization and integration with experimental proteomic data. *Bioinformatics* 30 (2014) 884-886.
- [9] L. Zimmermann, A. Stephens, S.Z. Nam, D. Rau, J. Kübler, M. Lozajic, F. Gabler, J. Söding, A.N. Lupas, V. Alva. A completely reimplemented MPI Bioinformatics toolkit with a new HHpred server at its core. *J. Mol. Biol.* 430 (2018) 2237-2243.
- [10] W.G. Touw, C. Baakman, J. Black, T.A. te Beek, E. Krieger, R.P. Joosten, G. Vriend. A series of PDB-related databanks for everyday needs. *Nucleic Acids Res.* 43 (2015) D364-D368.
- [11] L. Holm, L.M. Laakso. Dali server update. *Nucleic Acids Res.* 44 (2016) W351-W355.
- [12] T. Madej, C.J. Lanczycki, D. Zhang, P.A. Thiessen, R.C. Geer, A. Marchler-Bauer, S.H. Bryant. MMDB and VAST+: tracking structural similarities between macromolecular complexes. *Nucleic Acids Res.* 42 (2014) D297-D303.
- [13] S. Kumar, G. Stecher, K. Tamura. MEGA7: Molecular Evolutionary Genetics Analysis version 7.0 for bigger datasets. *Mol. Biol. Evol.* 33 (2016) 1870-1874.
- [14] D.T. Jones, W.R. Taylor, J.M. Thornton. The rapid generation of mutation data matrices from protein sequences. *Comput. Appl. Biosci.* 8 (1992) 275-282.
- [15] R.C. Edgar. MUSCLE: multiple sequence alignment with high accuracy and high throughput. *Nucleic Acids Res.* 32 (2004) 1792-1797.
- [16] U. Römling, Z. Bian, M. Hammar, W.D. Sierralta, S. Normark. Curli fibers are highly conserved between *Salmonella typhimurium* and *Escherichia coli* with respect to operon structure and regulation. *J. Bacteriol.* 180 (1998) 722-731.
- [17] U. Römling, W.D. Sierralta, K. Eriksson, S. Normark. Multicellular and aggregative behaviour of *Salmonella typhimurium* strains is controlled by mutations in the *agfD* promoter. *Mol. Microbiol.* 28 (1998) 249-264.

- [18] X. Zogaj, M. Nimtz, M. Rohde, W. Bokranz, U. Römling. The multicellular morphotypes of *Salmonella typhimurium* and *Escherichia coli* produce cellulose as the second component of the extracellular matrix. *Mol. Microbiol.* 39 (2001) 1452-1463.
- [19] I. Ahmad, S.F. Rouf, L. Sun, A. Cimdins, S. Shafeeq, S. Le Guyon, M. Schottkowski, M. Rhen, U. Römling. BcsZ inhibits biofilm phenotypes and promotes virulence by blocking cellulose production in *Salmonella enterica* serovar Typhimurium. *Microb. Cell Fact.* 15 (2016) 177.
- [20] L.M. Guzman, D. Belin, M.J. Carson, J. Beckwith. Tight regulation, modulation, and high-level expression by vectors containing the arabinose P_{BAD} promoter. *J. Bacteriol.* 177 (1995) 4121-4130.
- [21] I. Ahmad, A. Cimdins, T. Beske, U. Römling. Detailed analysis of c-di-GMP mediated regulation of *csgD* expression in *Salmonella typhimurium*. *BMC Microbiol.* 17 (2017) 27.
- [22] B. Staskawicz, D. Dahlbeck, N. Keen, C. Napoli. Molecular characterization of cloned avirulence genes from race 0 and race 1 of *Pseudomonas syringae* pv. *glycinea*. *J. Bacteriol.* 169 (1987) 5789-5794.
- [23] K.A. Datsenko, B.L. Wanner. One-step inactivation of chromosomal genes in *Escherichia coli* K-12 using PCR products. *Proc. Natl. Acad. Sci. USA* 97 (2000) 6640-6645.
- [24] S. Uzzau, N. Figueroa-Bossi, S. Rubino, L. Bossi. Epitope tagging of chromosomal genes in *Salmonella*. *Proc. Natl. Acad. Sci. USA* 98 (2001) 15264-15269.
- [25] R. Simm, M. Morr, A. Kader, M. Nimtz, U. Römling. GGDEF and EAL domains inversely regulate cyclic di-GMP levels and transition from sessility to motility. *Mol. Microbiol.* 53 (2004) 1123-1134.
- [26] Z. Zhou, A.A. Ribeiro, S. Lin, R.J. Cotter, S.I. Miller, C.R. Raetz. Lipid A modifications in polymyxin-resistant *Salmonella typhimurium*: PmrA-dependent 4-amino-4-deoxy-L-arabinose, and phosphoethanolamine incorporation. *J. Biol. Chem.* 276 (2001) 43111-43121.
- [27] H. Lee, F.F. Hsu, J. Turk, E.A. Groisman. The PmrA-regulated *pmrC* gene mediates phosphoethanolamine modification of lipid A and polymyxin resistance in *Salmonella enterica*. *J. Bacteriol.* 186 (2004) 4124-4133.
- [28] C.M. Reynolds, S.R. Kalb, R.J. Cotter, C.R. Raetz. A phosphoethanolamine transferase specific for the outer 3-deoxy-D-manno-octulosonic acid residue of *Escherichia coli* lipopolysaccharide. Identification of the *eptB* gene and Ca²⁺ hypersensitivity of an *eptB* deletion mutant. *J. Biol. Chem.* 280 (2005) 21202-21211.
- [29] R. Tamayo, B. Choudhury, A. Septer, M. Merighi, R. Carlson, J.S. Gunn. Identification of *cptA*, a PmrA-regulated locus required for phosphoethanolamine modification of the *Salmonella enterica* serovar *typhimurium* lipopolysaccharide core. *J. Bacteriol.* 187 (2005) 3391-3399.
- [30] S. Bontemps-Gallo, V. Coge, C. Robbe-Masselot, K. Quintard, J. Dondeyne, E. Madec, J.M. Lacroix. Biosynthesis of osmoregulated periplasmic glucans in *Escherichia coli*: the phosphoethanolamine transferase is encoded by *opgE*. *Biomed. Res. Int.* 2013 (2013) 371429.
- [31] M. Doumith, G. Godbole, P. Ashton, L. Larkin, T. Dallman, M. Day, B. Muller-Pebody, M.J. Ellington, E. de Pinna, A.P. Johnson, K.L. Hopkins, N. Woodford. Detection of the plasmid-mediated *mcr-1* gene conferring colistin resistance in

- human and food isolates of *Salmonella enterica* and *Escherichia coli* in England and Wales. *J. Antimicrob. Chemother.* 71 (2016) 2300-2305.
- [32] X. Lu, Y. Hu, M. Luo, H. Zhou, X. Wang, Y. Du, Z. Li, J. Xu, B. Zhu, X. Xu, B. Kan. MCR-1.6, a new MCR variant carried by an IncP plasmid in a colistin-resistant *Salmonella enterica* serovar Typhimurium isolate from a healthy individual. *Antimicrob. Agents Chemother.* 61 (2017) e02632-02616.
- [33] A.A. Bhagwat, P. Kannan, Y.N. Leow, M. Dharne, A. Smith. Role of anionic charges of osmoregulated periplasmic glucans of *Salmonella enterica* serovar Typhimurium SL1344 in mice virulence. *Arch. Microbiol.* 194 (2012) 541-548.
- [34] H. Dong, Z. Zhang, X. Tang, S. Huang, H. Li, B. Peng, C. Dong. Structural insights into cardiolipin transfer from the Inner membrane to the outer membrane by PbgA in Gram-negative bacteria. *Sci. Rep.* 6 (2016) 30815.
- [35] T. Nugent, D.T. Jones. Detecting pore-lining regions in transmembrane protein sequences. *BMC Bioinform.* 13 (2012) 169.